Journal of Inclusion Phenomena and Molecular Recognition in Chemistry **12**: 23–53, 1992.

Free Energy Perturbation Simulations of Cation Binding to Valinomycin

GEORGE EISENMAN*
Department of Physiology, UCLA Medical School, Los Angeles, CA 90024-1751, U.S.A.

OSVALDO ALVAREZ
Department of Biology, Faculty of Sciences, University of Chile, Santiago, Chile.

JOHAN AQVIST
Department of Molecular Biology, Uppsala Biomedical Center, S-75124 Uppsala, Sweden.

(Received: 27 September 1990; in final form: 11 December 1990)

Abstract. Experimental values of the free energies of cation binding to the cyclic depsipeptide molecule, valinomycin, obtained from Pedersen-type salt extraction measurements, provide data against which it is possible to test the adequacy of the procedures and force fields of the molecular dynamics algorithms, MOLARIS and GROMOS. These data are then used to assess appropriate values for the partial charges of the ester carbonyl oxygen and carbon. Valinomycin was chosen because it has only one kind of ion-binding ligand and because the cation is sufficiently enfolded by the molecule in the ion-complexes that the overall size and shape of the complex is virtually the same regardless of the species of cation bound. For such an 'isosteric complex', the experimentally measured selectivities are sufficiently similar in a wide variety of solvent environments that the *differences* in free energies measured between the different ion-valinomycin complexes by two-phase salt extraction experiments into dichloromethane can be taken as equivalent to the differences in free energies *in vacuo*. These *differences* were therefore compared with those computed for ion-valinomycin complexation *in vacuo* by Free Energy Perturbation/Molecular Dynamics (FEP/MD) simulations using the MOLARIS and GROMOS programs. Starting with a set of Lennard-Jones 6–12 parameters for the monovalent cations assessed for aqueous solution we explored the effect of varying the partial charges of the ester carbonyl ligands on binding free energy differences (i.e. the selectivity) among Na, K, Rb, and Cs. The computed selectivity was found to depend strongly on the value of partial charge, following a typical 'Eisenman Selectivity Pattern' in which the correct selectivity sequence and magnitude occurred only over a very narrow range of partial charge (around 0.33 and 0.6 for the standard carbonyls of MOLARIS and GROMOS, respectively). Using MOLARIS we explored the effect of varying the size of the ester carbonyl ligands by comparing the standard carbonyl of MOLARIS with the somewhat smaller carbonyls of GROMOS and found an equally satisfactory ability to reproduce the experimental data with a partial charge value of 0.41. These results validate the use of both the MOLARIS and GROMOS force fields as starting points for quantitative calculations of ion-binding in more complex molecules (e.g., ion-binding sites and channels in proteins).

Key words. Molecular dynamics, free energy perturbation simulations, ion-binding ion-complexation, ion-selectivity, ion-carbonyl bond angles and distances, valinomycin selectivity, MOLARIS, GROMOS, Pedersen two-phase salt-extraction, Eisenman selectivity sequences, Lennard-Jones parameters for ions, isostericity.

This paper is dedicated to the memory of the late Dr C. J. Pedersen.
* Author for correspondence.

1. Introduction

Charles Pedersen discovered the first synthetic neutral compounds, the crown ethers, that formed stable complexes with alkali metal cations [1]. The importance of these molecules as model compounds for ion carriers in membranes, and their fundamental similarity to the neutral antibiotic ion carriers like valinomycin and monactin was immediately recognized [2]. Indeed, the first author had the pleasure in 1968 of inviting Pedersen to present his work to the American Physiological Society Symposium on 'Biological and Artificial Membranes' [3]. Pedersen's pioneering work provided a crucial system in which to confront classical chemical concepts and measurements with those of the newly opened field of ion permeation in lipid bilayer membranes. It played a central role in establishing a rigorous understanding of the chemistry underlying the effects of macrocyclic carrier molecules on bilayer membranes [4–6] and ultimately proved to be central in clarifying a number of fundamental assumptions regarding the stoichiometry of membrane carriers [7]. Understanding how ions selectively interact with his molecules is still fundamental to understanding ion binding to the peptide backbone, a central feature of ion binding sites in protein enzymes and channels.

It seems particularly appropriate to dedicate the present paper to Charlie Pedersen, since at the aforementioned Symposium Pedersen described the two-phase salt extraction procedure for measuring free energies of ion binding [3] which will be used here, some 22 years later, to measure experimental free energies of ion-binding to valinomycin for comparison with those computed by free energy perturbation (FEP) simulations. These experimental data enable a test to be made of the validity of the procedures and force fields of molecular dynamics for simulating selective ion binding to a peptide-like molecule. These data also provide a basis for assigning appropriate values for the partial charges of the carbonyl group.

The present contribution represents a small step directed towards a central problem in molecular biophysics, namely how to assess the energetics of specific interactions between ions and proteins. These energies determine the affinities and rates of ion binding, unbinding and permeation for protein channels as well as for ion-activated enzymes. Recent advances in computational power available on laboratory minisupercomputers together with great progress in developing appropriate force fields and algorithms for the computational chemistry of proteins [8–12] offer the promise of being able to deduce details of channel permeation from structural knowledge, and vice versa. Examples of channels for which calculations have been performed are the gramicidin channel [13, and references therein], the acetylcholine receptor channel [14–16] and certain channel-like structures in the protein coat of icosahedral viruses [17–18]. Relevant calculations of the affinity of crown ethers and other small ion-binding molecules [19–21], of specific ion binding to proteins [22], and to specific ion effects on catalysis [23] are also encouragingly reasonable.

Despite the apparent adequacy of the force fields used, as judged by ability to generate correct protein structures [24–27], the use of molecular dynamics simulations to calculate the specific interactions of ions with protein binding sites is still in an early stage. In particular, no algorithm has yet been tested for any molecule

whose ion-binding selectivity and three-dimensional structure are *both* known. Indeed, only very recently has a reliable set of Lennard-Jones 6–12 ion-water interaction parameters been derived for the Group Ia and IIa cations from free energy simulations [28] in bulk water. This set of parameters was derived by performing free energy perturbation simulations at 298 K of the process of charging an ion in aqueous solution. The model system consisted of an ion, described as a point charge imbedded in Lennard-Jones spheres characterized by the A and B parameters, surrounded by a surface constrained drop of explicit (flexible or rigid) SPC water molecules. The oxygen Lennard-Jones A and B parameters were 793.3 and 25.01. The computations produced the observed absolute hydration free energies and the radial distribution function of water around the ions. The A and B parameters for the monovalent cations are listed in Section 4.2 'General Procedure'. These parameters are the starting point for the present study of ion binding to a prototype ion-binding ligand, the ester carbonyl group of the backbone of the cyclic depsipeptide ion-carrying molecule, valinomycin.

Such carbonyls are important ligands in many cation binding sites in proteins [29–31]. Indeed, backbone amide carbonyls are the sole ligands in the five-fold ion binding site of the satellite tobacco necrosis virus [32, 33] and the gramicidin channel [34, 35]. We show here that the experimental selectivity data and structure for valinomycin can indeed be described by molecular dynamics procedures such as the MOLARIS force field [9, 36, 37], provided the carbonyl partial charges are appropriately parametrized. Our results suggest that the partial charge parameters computed here can serve as a useful starting point for refining previous computations of free energies of ion interactions with the amide carbonyl ligands in more complex protein structures such as the Gramicidin channel [13] and the five-fold Ca binding site in the satellite tobacco necrosis virus [18, 22, 38]. When appropriate account is taken of variable stoichiometry, structure, and hydration, quantitative calculations for ion complexes with Pedersen's crown compounds should also become feasible.

This contribution has been adapted from a paper presented to the Royal Society of Chemistry Faraday Symposium No. 26 'Molecular Transport in Confined Regions and Membranes', University of Oxford, England, Dec. 17–18, 1990; and the analysis of structure and selectivity has been considerably extended.

2. Valinomycin Structure

The primary structure of valinomycin is

cyclo-(D-HYL-D-VAL-L-LAC-L-VAL-)$_3$

where D-DYL is D-hydroxyisovaleric acid, L-LAC is L-lactic acid, and D-VAL and L-VAL are D- and L- valine, respectively. The atom types, standard partial charges, and Lennard-Jones A and B parameters used in MOLARIS are given in Figure 1.

In low dielectric constant solvents, as well as in the crystalline cation complexes, the valinomycin molecule wraps around a cation to form a bracelet shaped structure in which the ion is liganded by six ester carbonyl oxygens and which is stabilized by six intramolecular H-bonds between all the —NH groups and the

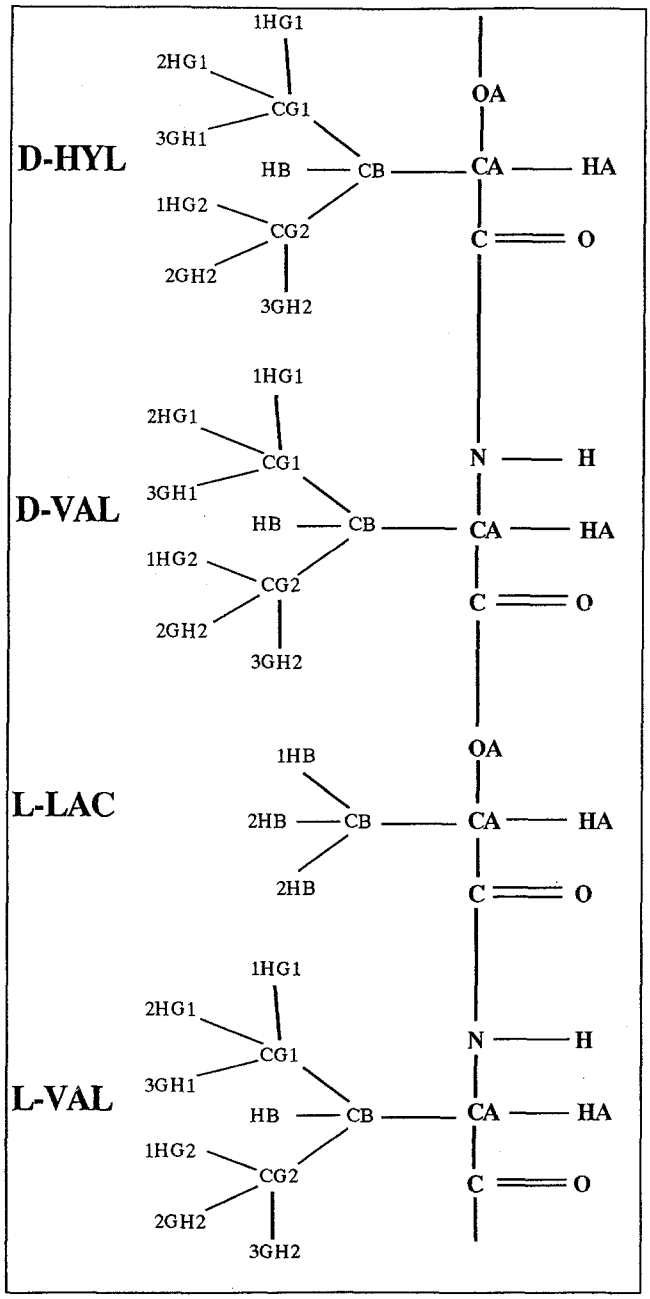

OA (Hyl and Lac)
Partial charge -0.400
A 793.30 B 25.00

CA (Hyl and Lac)
Partial charge 0.300
A 1956.00 B 32.00

HA (Hyl and Lac)
Partial charge 0.100
A 22.00 B 1.00

C
Partial charge 0.550
A 1956.00 B 32.00

O
Partial charge -0.550
A 793.30 B 25.00

N (VAL)
Partial charge -0.400
A 900.00 B 42.00

H (Val)
Partial charge 0.400
A 4.00 B 0.00

CA (Val)
Partial charge -0.097
A 1956.00 B 32.00

HA (Val)
Partial charge 0.097
A 22.00 B 1.00

CB (Hyl, Val)
Partial charge -0.097
A 1956.00 B 32.00

CB(Lac) CG1, CG2
Partial charge -0.291
A 1956.00 B 32.00

1HB, 2HB, 3HB, 1HG1, 2HG1, 3HG1, 1HG2, 2HG2, 3HG2
Partial charge 0.097
A 22.00 B 1.00

Fig. 1. Valinomycin chemical structure and atom types. The Lennard-Jones 6–12 A and B parameters and partial charges used in Amino88 amino acid library for MOLARIS are indicated at the right.

amide carbonyl oxygens (see Ovchinnikov *et al.* [39] for review of the extensive conformation studies). One face of the structure is formed by D-HYL, the other by L-LAC. The three-dimensional structure of the K complex in the bis-(Valinomycin) potassium tri-iodide penta-iodide crystal has been determined (including hydrogens by Neupert-Laves and Dobler [40]) and is available as the Cambridge Data Bank structure VALINK. Structures without H atoms are also available for the Cs picrate complex and the Na picrate monohydrate *m*-xylene solvate complex (Cambridge codes: DOWDAU [41] and BINFIN [42], respectively).

The crystallographic coordinates of the three-dimensional structure of VALINK were converted using the ability of the Biodesign BIOGRAF program to read a Cambridge format file, make the connections of the atom using geometrical rules, and create an intermediate file in which the atoms are segregated by type, rather than by residue, but in which their connections are given explicitly. To make the final Brookhaven format file for input to MOLARIS, the identity of each atom in the intermediate file was deduced from the connections, the atoms were grouped by residues and the ring was closed by hand-connecting the carbonyl carbon of VAL-12 with the hydroxyl oxygen of HYL-1. For computations all the iodide data were deleted.

3. Calculation of Free Energies for Binding Ions to Valinomycin *in vacuo*

Well-defined free energy *differences* among the alkali metal cations in their interactions with valinomycin can be measured in several ways: (1) by two-phase salt-extraction equilibria [3–6]; (2) by ion complexation equilibria in a single phase [43]; (3) by effects on the electrical conductance and permeability of lipid bilayers [44, 5, 6]; and (4) by the electrical potentials of thick ion-selective electrodes [45]. The free energy differences are directly related to the ratios between species I^+ and J^+ of their two-phase equilibrium constants (K_I/K_J), their one-phase complexation constants (K_{Is}/K_{Js}), their membrane permeabilities (P_I/P_J), their membrane conductances (G_I/G_J), and their electrode selectivities (S_I/S_J).

3.1. THEORETICAL EXPECTATIONS FOR ISOTERIC COMPLEXES

The following approximate identity is theoretically expected [4–6] to relate to the above ratios for 'isosteric complexes' in which the overall size, shape, and charge distribution of the complex are the same regardless of the species of ion complexed:

$$K_I/K_J = K_{Is}/K_{Js} = P_I/P_J = G_I/G_J = S_I/S_J \tag{1}$$

Equation (1) is exact for exactly isosteric complexes; and we will present evidence below that it holds surprisingly well for valinomycin. The results presented here show that valinomycin-ion complexes are exactly isosteric for K and all larger ions, and quite isosteric for Na. The importance of this is that the free energy difference calculated between any pair of these ions by any of these measurements should depend only on the energy of complex formation *in vacuo* relative to the experimentally known free energies of ionic hydration. This enables us to use experimentally measured selectivity data to check the energies calculated by molecular dynamics (MD) simulations using the free energy perturbation (FEP) procedure.

3.2. EXPERIMENTAL RESULTS

We summarize here some results of a study of ion-valinomycin complexation (Gomez-Lojero and Eisenman, to be published) which are more extensive and precise than those previously reported [5, 6]. Figure 2 shows an example of typical

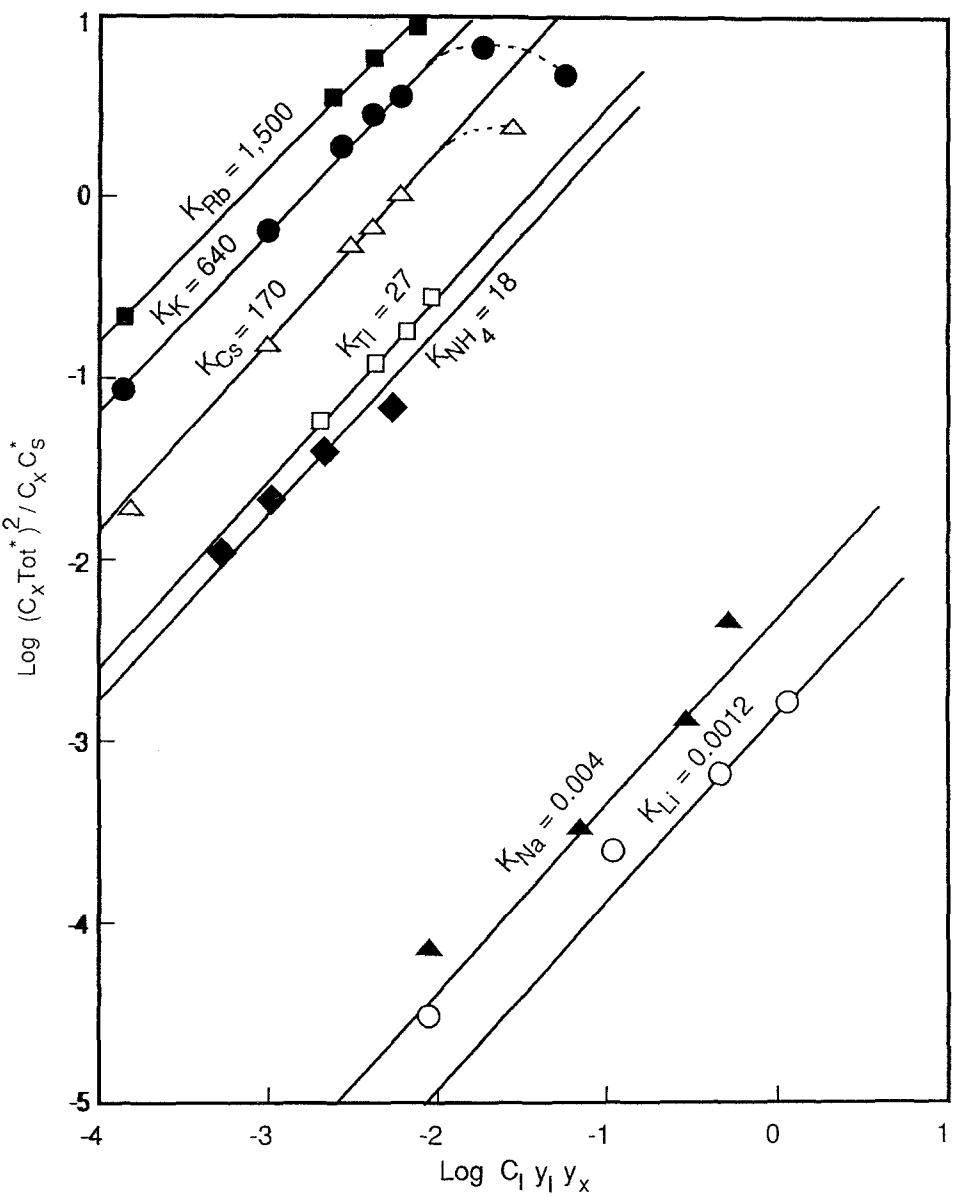

Fig. 2. Equilibrium extraction of 2,4-dinitrophenolates of the indicated cations by valinomycin into dichloromethane. The data are plotted in logarithmic form according to the expectations of Equation (50) of Ref. [4] in the manner of Figure 7 of that reference. The ordinate is dimensionless; the concentrations are in moles/liter and y's are molar activity coefficients. The slope of the lines = 1.

data for the extraction by valinomycin into dichloromethane for the 2,4-DNP salts and demonstrates that the behavior is consistent with the chemistry of forming 1:1 ion-complexes in this solvent uncomplicated by ion-pairing with the 2,4-DNP anion. The behavior is seen to be as regular as that previously found for the macrotetralide actins [4].

Figure 3 shows, for all cations except Li^+, that the equilibrium constant ratio K_I/K_J is independent of the anion, a finding which is only expected for isosteric complexes. This indicates that only the Li^+ complex is seriously non-isosteric, which is probably a consequence of the ability of the small Li ion to move away from the center of the complex toward its surface, as well as the possibility that a water molecule might be included in the complex. There is evidence in *n*-hexane that Li, and to a lesser extent Na, could move toward the surface of the complex under the influence of an adjacent anion to form a 'tight' ion pair. In *n*-hexane a blue shift in the picrate UV absorbance spectrum has been found for Li and Na (Gomez-Lojero and Eisenman, unpublished results) despite the absence of any such shift for the complexes of the larger ions, which are strictly isosteric even in *n*-hexane. Clearly, Li (and to a lesser extent, Na) are not as well screened from the picrate as the larger cations. For this reason, and because there is room within the valinomycin-Li complex for a water molecule, we will exclude Li from the quantitative comparisons.

Figure 4 illustrates the effect of varying the dielectric constant of the solvent (from a value of less than 2 in *n*-hexane to more than 9 in dichloromethane) on the salt extraction equilibrium constants. Despite the huge dependence of K_I on the dielectric constant, the independence of the ratios between ions is apparent from the parallelism of the lines. This behavior indicates that the selectivity (i.e. the difference in free energies) is completely independent of the dielectric constant.

This conclusion is further supported by the results of Figure 5, which show a very close agreement between the ratios of heterogeneous ion-complexation constants (K_I/K_K) measured by two-phase salt extraction equilibria into dichloromethane and the ratios of single-phase ion-complexation constants (K_{Is}/K_{Ks}) measured in methanol by Grell *et al.* [43]. Measurements for Li^+ complexation in methanol do not exist, and only for Na^+ is there any detectable deviation from the straight line expected for strict isostericity between these two extremely different solvent environments.

These results are summarized in Tables I and II. Table I compares the equilibrium constants measured for two-phase salt extraction into three different solvent mixtures: pure dichloromethane, a 64% *n*-hexane–36% dichloromethane mixture, and pure *n*-hexane. It can be seen in this table that, although the absolute value of the heterogeneous equilibrium constant decreases by a factor of 10 000 000 on lowering the dielectric constant (cf. the value of K_K of 52 000 in CH_2Cl_2 vs. 0.00044 in *n*-hexane), the ratios $K_I K_{Cs}$ is remarkably species independent, as can be seen by the constancy of values of the K_K/K_{Cs} and K_{Rb}/K_{Cs} ratios, which vary by less than 25%.

Table II extracts the free energy differences for exchanging an ion for K^+ relative to the aqueous reference state. Column 1 summarizes the equilibrium constants reported previously for dichloromethane [5]; while column 2 summarizes the more accurate ones from the first row of Table I. These values are used to calculate the

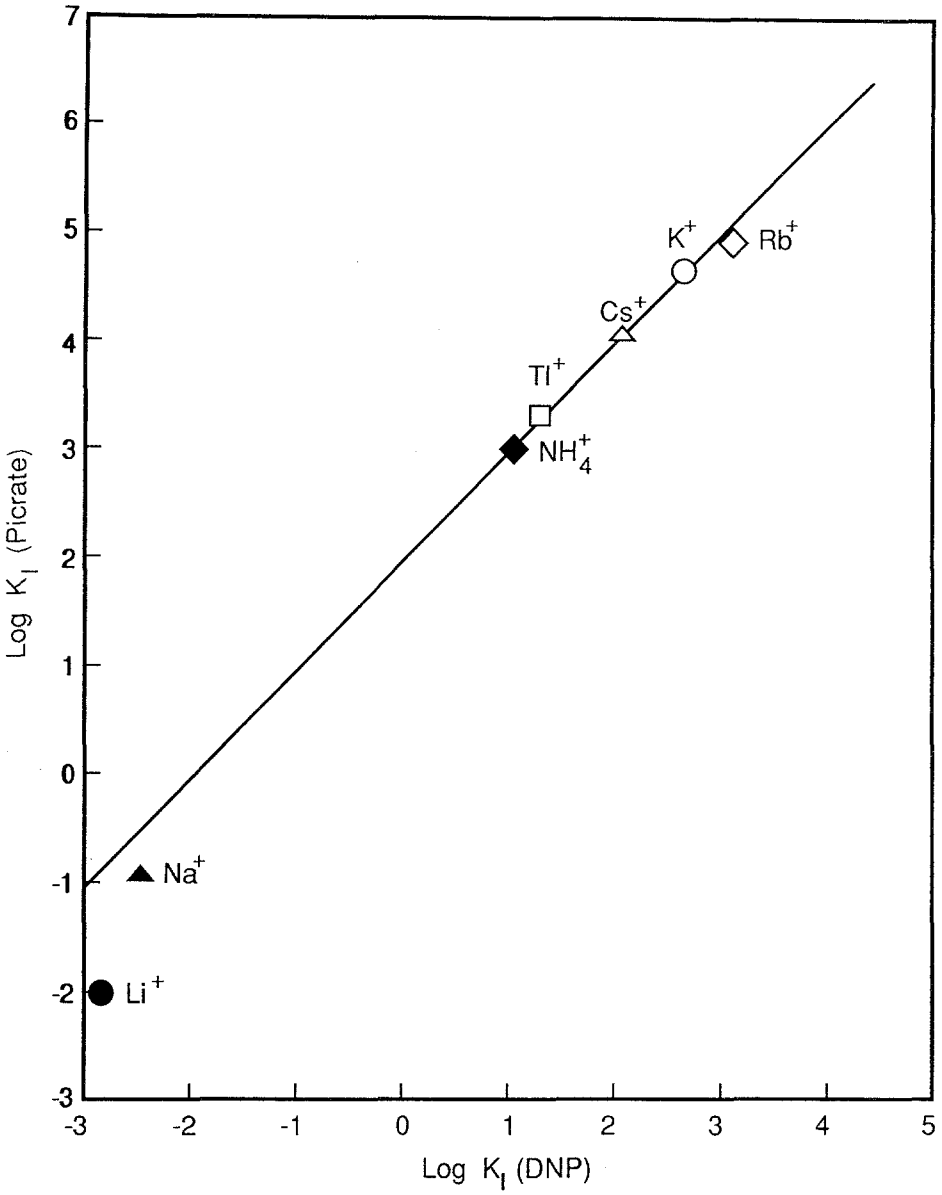

Fig. 3. Correlation between absolute values of salt extraction equilibrium constants for valinomycin in dichloromethane for picrates (ordinate) vs 2,4-dinitrophenolates (abscissa). Unpublished data of Gomez-Lojero and Eisenman. The line is drawn with a slope of 1.

ratios K_I/K_K in the third column. The last column summarizes the free energy differences corresponding to these. We will use these values as a measure of the difference in free energy of the reaction to form the complex *in vacuo* relative to the experimental free energies of hydration. The validity of this rests only on the assumption that the energy of interaction of the complex with any medium external to it is independent of the species of ion complexed (i.e. is independent of the

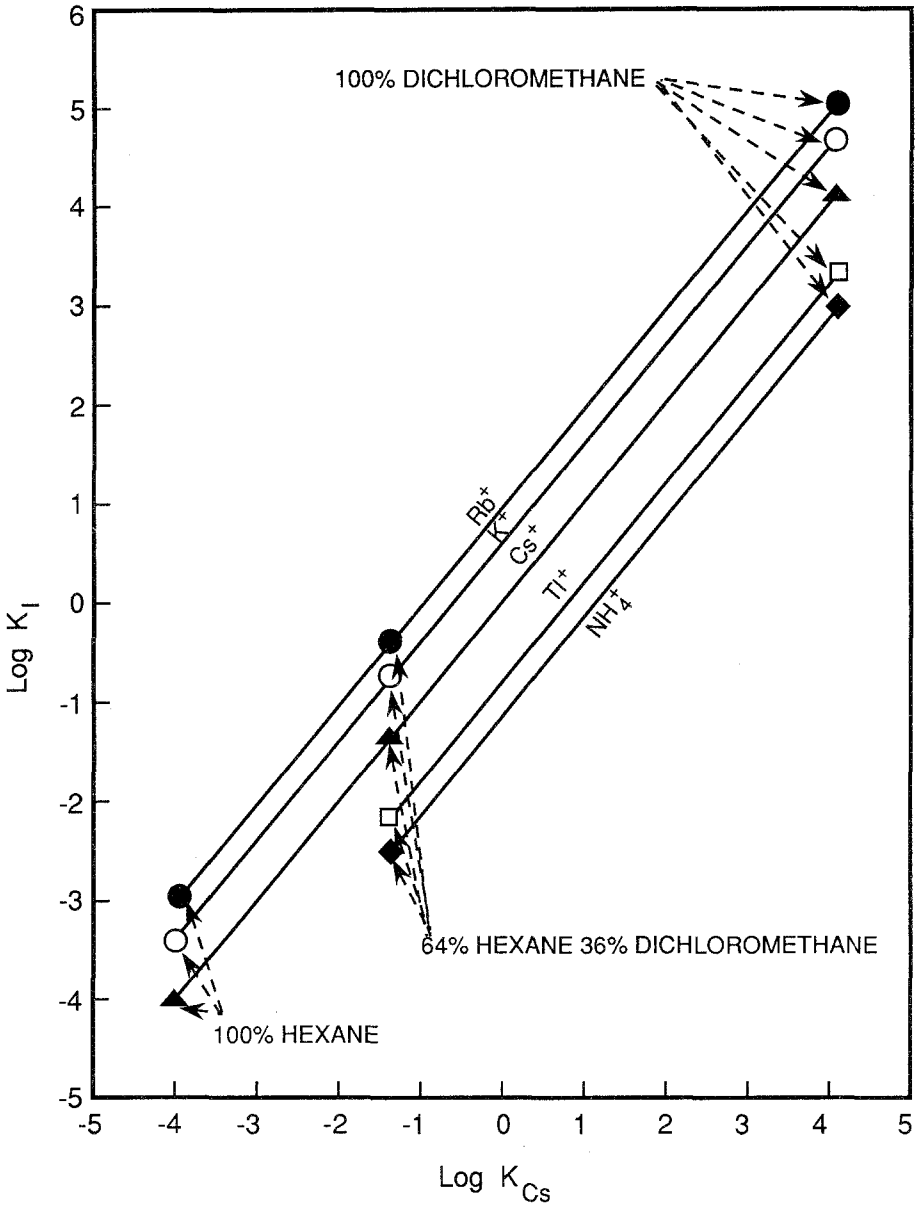

Fig. 4. Demonstration of the independence of the ratios of two-phase equilibrium constants of the nature and dielectric constant of the solvent as this is varied from hexane to dichloromethane. The effect of varying the solvent on the values of $\log_{10} K_1$ are plotted against $\log_{10} K_{Cs}$. Unpublished data of Gomez-Lojero and Eisenman.

dielectric constant of the solvent (and even of its chemical nature). This is so because when computing the free energy differences, the conformations of the uncomplexed valinomycin cancel out, as do the energies of interaction of isosteric complexes with the medium [6].

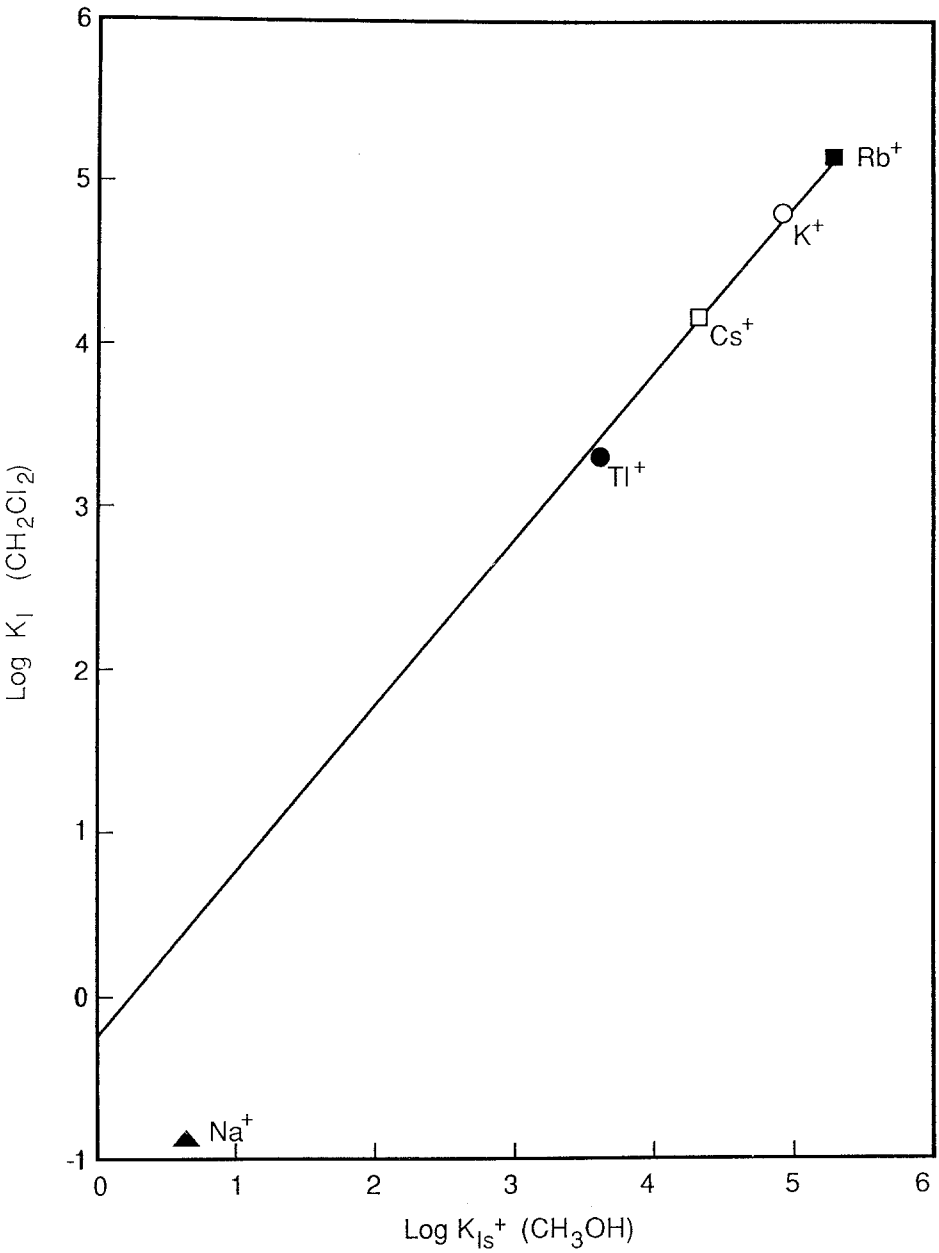

Fig. 5. Correlation between salt extraction constants into dichloromethane (ordinate) from Table I and stability constants in methanol (abscissa) [41]. Only Na^+ deviates from the line of slope 1 expected for perfect isostericity.

Table I. Equilibrium constants of picrate with valinomycin

Equilibrium Constants	Solvent	Li	Na	K	Rb	Cs	NH_4	Tl
K_I	CH_2Cl_2	0.0098	0.13	52 000	110 000	14 500	1200	2400
	64% hexane–36% CH_2Cl_2			0.14	0.25	0.031	0.0037	0.0064
	hexane			0.00044	0.001	0.0001		
K_I/K_{Cs}	CH_2Cl_2	0.00000067	0.000009	3.54	7.6	1	0.082	0.165
	64% hexane–36% CH_2Cl_2			4.5	8	1	0.12	0.2
	hexane			4.4	10	1		

Table II. Salt extraction equilibrium constants (K_I), their ratios (K_I/K_K), and the differences in free energies of exchanging ((ΔF_{exch})(I_K)) an ion for K^+ (relative to the aqueous standard state)

	K_I^a	K_I	K_I/K_K	$\Delta F_{exch}(I_K)$
Li	0.07	0.0098	0.00000019	+9.17 kcal
Na	0.18	0.13	0.0000025	+7.64
K	10 400	52 000	1.0	0
Rb	20 500	110 000	2.147	−0.45
Cs	6450	14 500	0.2825	+0.75
NH_4	2000	1200	0.0232	+2.23
Tl	—	2400	0.0466	+1.82

[a]Eisenman *et al.* [5]

Notice in Table II that the selectivity sequence is Rb > Cs > K ⋙ Na > Li, which is Eisenman selectivity sequence III [46, 47], and that there is a large, 7.64 kcal, difference in selectivity favoring K over Na. Satisfying these two observations is the task of any theoretical algorithm that is to be relied upon for inferring ion-protein interactions. We will test the MOLARIS [36] and GROMOS [25] algorithms here.

3.3 OTHER SIGNS OF ISOSTERICITY

Table III compares the ratios of salt extraction equilibrium constants from Table II with selectivity ratios determined in four other measurements: complexation constants in methanol [43], permeability ratios in bilayers (Krasne and Eisenman, unpublished data), conductance ratios in bilayers [44], and bulk phase electrode selectivities [45]. All measurements agree that the selectivity sequence is Rb > K > Cs ⋙ Na > Li; and the agreement can be seen in Table III to be satisfactorily quantitative, given the technical difficulty of measuring very small values of permeability and conductance ratios in bilayers. As discussed elsewhere [5, 6] such agreement is only expected for isosteric complexes.

Table III. Comparisons of ratios of salt extraction equilibrium constants (K_I/K_K), complexation constants (K_{Is}/K_{Ks}) in methanol, permeability ratios (P_I/P_K) in bilayers, conductance ratios (G_I/G_K) in bilayers, and selectivity ratios (S_I/S_K) in ion selective electrodes

	K_I/K_K	K_{Is}/K_{Ks}^a	p_I/p_K^b	G_I/G_K^c	S_I/S_K^d
Li	0.00000019	—	0.0000047	<0.005	<0.00021
Na	0.0000025	0.00016	0.000036	<0.006	<0.00026
K	1.0	1.0	1.0	1.0	1.0
Rb	2.147	2.17	1.8	1.5	1.9
Cs	0.2825	0.267	0.76	0.25	0.48

[a]Grell, *et al.* [43], Table VII.
[b]Unpublished data of Krasne and Eisenman for glycerol monooleate bilayers.
[c]Mueller and Rudin [44], at 35°C and 0.05 M salt.
[d]Pioda *et al.* [45] in diphenyl ether.

3.4. FREE ENERGY DIFFERENCES OF VALINOMYCIN–ION COMPLEX *IN VACUO*

The differences in free energy of binding of the various ions to valinomycin *in vacuo* can be calculated from ΔF_{exch} in Table II by subtracting from these the experimentally known differences in free energy of hydration [48]. The free energy of exchange, ΔF_{exch}, relative to Cs^+ from Table II are:

Li^+	8.42 kcal/M
Na^+	6.89
K^+	−0.75
Rb^+	−1.20
Cs^+	0

The free energies of hydration and the binding energy differences *in vacuo* are:

	$\Delta F_{hydration}$[48]	$\Delta F_{binding}$
Li	−54.3	−45.88
Na	−30.4	−23.31
K	−12.8	−13.55
Rb	−7.7	−8.9
Cs	0.0	0.0

The absolute values of these latter energies are seen to be monotonically increasing functions of decreasing ionic radius. The selectivity implicit in these will be examined in a later section.

4. Computations

4.1 MOLECULAR DYNAMICS/FREE ENERGY PERTURBATION SIMULATIONS

Since the criterion of isostericity is fulfilled for the alkali ion-valinomycin complexes, one only needs to calculate the difference in free energy between the various ion complexes *in vacuo* to obtain the differential binding free energies and thus the selectivity properties of the host. Our strategy in all the reported calculations was therefore to start from the Na-valinomycin complex and in two separate runs slowly 'mutate' Na into K, Rb, and Cs in one run and into Li in another. (Additionally, we started from the Cs–valinomycin complex and slowly mutated Cs into Rb, K, and Na in one run and started from the Li complex and slowly mutated into the Na). During the process of mutation, the structure was allowed to rearrange and the overall free energy change of the system was recorded. All computations were carried out using the MOLARIS program [36] with its standard force fields and parameters (Amino88 library), except as specifically noted, to perform MD/FEP computations [49, 37]. The MOLARIS code was provided by Arieh Warshel and run on an Ardent Titan minisupercomputer.

4.2. GENERAL PROCEDURE

The crystallographic structure for the K^+–valinomycin complex of Neupert-Laves and Dobler [40] was first energy-minimized by 1 ps of molecular dynamics at 5 K with K^+ bound in order to remove possible bad contacts. The resulting atomic coordinates were used as the starting point for subsequent calculations and called the 'annealed structure'.

The free energy change of replacing one ion by another at 100 K was calculated by slowly 'mutating' the Lennard-Jones 6–12 parameters of one ion to another. In forward mutations from smaller to larger sized ions, K^+ in the annealed structure was replaced by Na^+ and subjected to 3 ps of molecular dynamics at 100 K to bring it into the Na^+ form. The Lennard-Jones parameters of the ion were then gradually 'mutated' from those for Na^+ to those for Cs^+ in 35 steps (the spacing between these steps was chosen for most efficient weighting of the energies), passing through K and Rb in the process. The reverse procedure started with replacing Cs^+ for K^+ in the annealed structure and performing 3 ps of molecular dynamics at 100 K to bring the complex into the Cs^+ form. In this way it is possible to obtain the free energy change for each of the ions (Na, K, Rb, and Cs) in one run since one passes through the intermediate sized ions on the way from the smaller to the larger and vice versa. K^+ corresponds to an ion that is 54% of the way from Na^+ to Cs^+; and Rb^+ to an ion that is 74% of the way from Na^+ to Cs^+. The reversibility of this procedure was verified and can be seen in Figure 6 and by comparing the top and bottom parts of Figure 7. A similar procedure was followed for the Na^+ to Li^+ and Li^+ to Na^+ mutations. The Lennard-Jones 6–12 parameters used for the ions [28] are given below.

	A_I	B_I
Li^+	30.2	2.66
Na^+	154.0	4.00
K^+	589.2	4.42
Rb^+	925.0	4.74
Cs^+	1830.0	5.60

At each of the 35 steps of a complete FEP/MD mutation a 1 ps trajectory was calculated, of which the last 0.6 ps were used for evaluating the overall free energy difference. The total free energy corresponding to a given mutation was obtained as the sum over the individual contributions from the 35 steps. For each step the free energy of 'moving' to the next point (i.e. of changing the effective MD potential by a small amount) was calculated as the Boltzmann average of a corresponding small perturbation to the potential energy function. Overall, a mutation run in 35 steps took about 33 hours of CPU time on one processor of an Ardent Titan minisupercomputer (viz. about 30 days to construct Figure 8). The total free energy change includes the cost of rearranging the host molecule and the non-bonded Coulomb and van der Waals interactions between the ion and the host. The present potential energy function does not include induced dipoles.

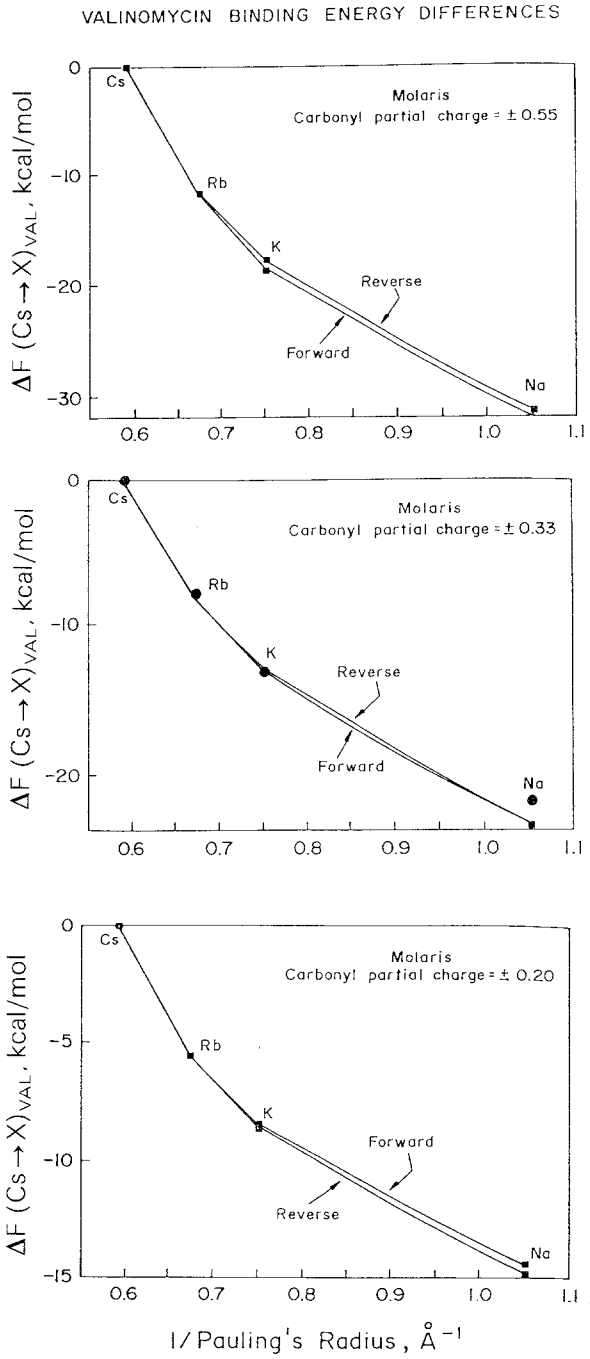

Fig. 6. Reversibility of FEP mutations in the forward (from Na to Cs) and backward (from Cs to Na) directions. Results for simulations for 3 different values of ester carbonyl partial charge are shown: $+/-0.55$, the default value for MOLARIS, at the top; $+/-0.20$ at the bottom; and $+/-0.33$, in the middle which gives the best agreement with the experimental values from salt extraction equilibria (indicated by experimental data points, the large dots in the middle figure).

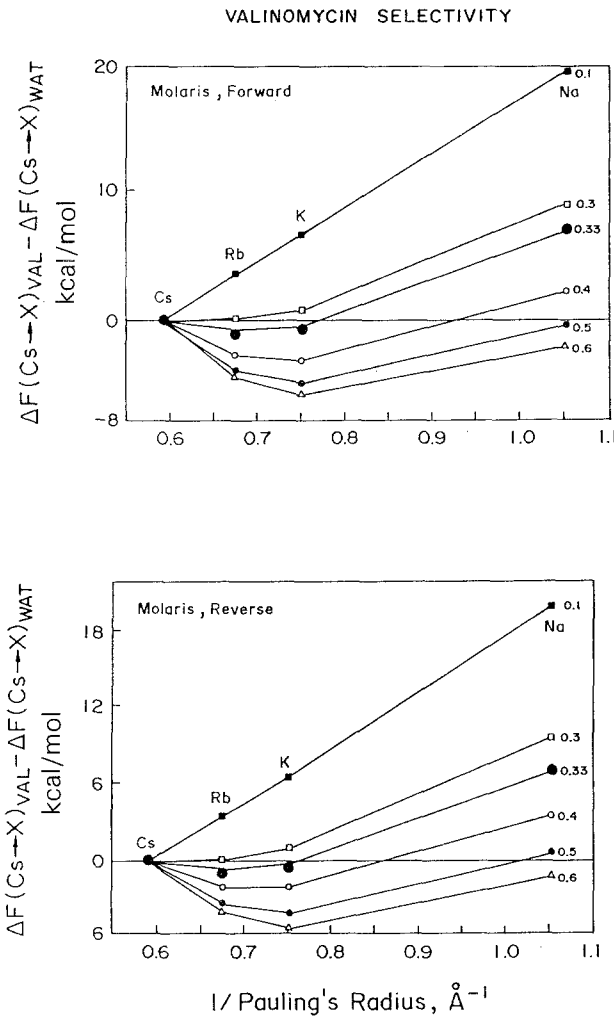

Fig. 7. Calculated values of free energy selectivity are plotted for the indicated values of ester carbonyl partial charge as a function of the reciprocal of the Pauling crystal radius for forward mutations (top) and reverse mutations (bottom). Selectivity is defined as the free energy difference between the ion–valinomycin complex and the Cs^+–valinomycin complex minus the difference in the experimental hydration free energy of the ion relative to Cs^+. Increasing selectivity is plotted downward. Experimental values are shown by the data points. Note the successive shift of selectivity optima from Cs^+ at a partial charge of 0.1, to Rb^+ at a partial charge of 0.33, and to K^+ at a partial charge of 0.5 or greater. This pattern is recognizable as having a 'Coulomb topology' [50]. The larger dots are experimental data.

4.3. CONSTRAINTS

We applied a very weak harmonic constraint of 0.1 kcal/Å^2 to the valinomycin atoms, which restrains them to their crystallographic structure. This constraint was included in order to compensate for the missing van der Waals' interaction with a surrounding (non-polar) solvent and because of uncertainties with respect to the torsional potentials. The magnitude of this constraint is so small that it is not likely

to have any influence on the present results and conclusions (for an atom that moves 1.0 Å the energy cost would only be 0.05 kcal/mol). We have recently reduced this constraint to zero in computations using GROMOS (see Section 6.2 of the Discussion) and have obtained results compatible with the results to be presented below.

4.4. RESULTS

4.4.1. *Reversibility*

Figure 6 demonstrates the reversibility of the MD/FEP procedure. The difference in free energy between Cs and the indicated cations *in vacuo* is plotted for the 'forward' mutation from Na to Cs and the 'reverse' mutation from Cs to Na as a function of the reciprocal of the Pauling crystal radius. The reversibility is shown for three different values of partial charge of the six ester carbonyl ion binding ligands. The top is the (high) default value (+0.55 for C, −0.55 for O) of the carbonyl partial charge for the standard (Amino88) parameters of MOLARIS. The bottom figure is for an extremely low value of partial charge (+/− 0.20). The middle is for a partial charge of +/− 0.33 which we will show below reproduces the experimental data for valinomycin quite well.

4.4.2. *Comparison of Computed Free Energies in vacuo with Experimental Values*

The differences in free energy of binding of the various ions to valinomycin *in vacuo* were calculated in Section 3.3. These 'experimental' *in vacuo* binding energies can now be directly compared with the *in vacuo* calculations by plotting the experimental values and noting how well these (solid dots) agree with the free energies for a partial charge of +/− 0.33 in the middle part of Figure 6.

4.4.3. *Selectivity: Comparison of Computated with Experimental Values*

Figure 7 shows the selectivity calculated by the MD/FEP procedure for the 'forward' mutation (top) and the 'reverse' mutation (bottom) for the indicated values of partial charge of the carbonyl ligand. For comparison, the experimental values of ΔF_{exch} recalculated from Table II relative to Cs^+ are plotted as large dots. It is apparent that the computed and experimental values agree quite satisfactorily for a value of partial charge of +/−0.33 and also that the minimum in the selectivity curve occurs at Rb for this value.

An alternative comparison is presented in Figure 8 which shows more clearly how the two experimental constraints on selectivity can be imposed to define quite narrowly the range of permissible values of carbonyl partial charge. It will be recalled that the first experimental constraint is that the selectivity sequence must be Rb > Kb > Cs ⩾ Na > Li. The top part of Figure 8 plots the free energy change for mutating a Na complex first into a K complex, then into a Rb complex, and finally into a Cs complex. The bottom part of Figure 8 plots the reverse process, mutating from larger to smaller ion. The Roman numerals indicate the ranges of carbonyl

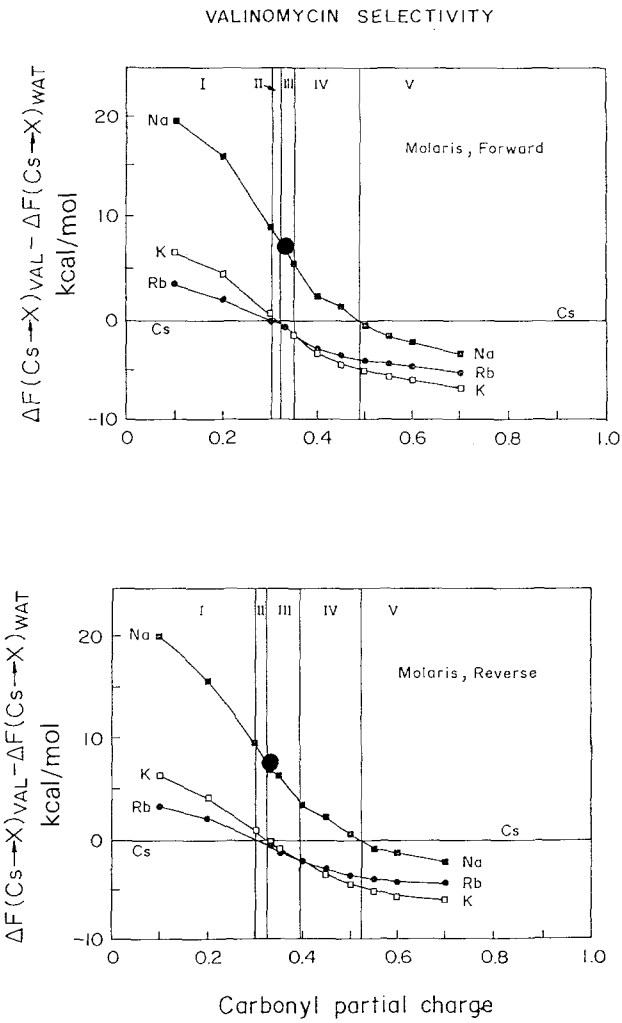

Fig. 8. Calculated values of free energy selectivity, defined as in Figure 7, are plotted as a function of the ester carbonyl partial charge for the indicated ions. Increasing selectivity is plotted downward. The intersections between the isotherms for each cation mark shifts in selectivity sequence, with the Roman numerals indicating the regions in which particular Eisenman sequences are seen. Experimental salt extraction data points for Na^+ (relative to Cs^+) are also plotted as a large dot at a partial charge of 0.33 for comparison with the Na^+ isotherm.

partial charge in which the Eisenman selectivity sequences corresponding to these numbers occur. They correspond to the regions between intersections of the isotherms for each ion.

It can be seen for both directions that there is a relatively narrow range of carbonyl partial charge, labelled 'III', in which the selectivity sequence Rb > K > Cs > Na is observed. This occurs in the region in which the Rb isotherm is the lowest, and, moreover, in the region where the K isotherm lies between the Rb and Cs isotherms (see below for more discussion of the selectivity pattern). If

we now apply the additional constraint that the free energy difference between Na and Cs must be 6.89 kcal/mol in favor of Cs we find that this indeed is satisfied within the sequence III region (compare experimental data point) with the Na isotherm and, moreover, that this occurs for a partial charge of 0.33 for both the forward and reverse mutations. In this way we have parameterized the ester carbonyl partial charge at a value of $+/-0.33$ for the standard Lennard-Jones 6–12 parameters of MOLARIS (see Figure 1) for the carbonyl oxygen and the alkali cations. In a subsequent section we will parameterize the partial change for the somewhat smaller carbonyl oxygen used by GROMOS [25].

The degree of quantitative agreement between computation and experimental data can be seen for each ion in Figure 7; but it is worth emphasizing the data plotted in Figure 9 which shows for both the forward and reverse mutations the very satisfactory agreement between experimental free energies (large filled circles) and the computed ones for a carbonyl particle charge of 0.33.

Finally, for completeness we show in Figure 10 the results for computations for Li in the reverse mutation (from Na to Li). As mentioned before, we will not try to compare these calculations with experimental data because it is highly likely that the Li^+ complex contains a water molecule and also because there are indications that 'tight' ion pairing between the Li and picrate ions make it difficult to interpret the salt extraction data. Briefly, whereas the computations indicate that Li should be highly disfavored to Na, the experiments indicate that the disfavoring is not as great. Such a difference between computed expectations and the observations of Tables II and III makes sense and probably can even be resolved quantitatively by extending the computations to allow a water molecule to enter the Li^+ complex.

4.4.4. *Parameterization of the C=O Partial Charge*

To our knowledge this constitutes the first test of a molecular dynamics simulations to reproduce *quantitatively* the free energies underlying ion-protein binding selectivity. It gives a strong indication that the MOLARIS force field, parameters, and procedure are adequate for ion-protein interactions. Of course, this has been tested only for the calculation of a free energy *difference* and needs to be extended to the calculation of the absolute values of free energy, which are known for the case of the ion-complexation constants measured by Grell *et al.* [43] for valinomycin in methanol (recall Table III), to which we plan to extend our computations. The partial charge value of 0.33 is much smaller than that used in MOLARIS for its standard amide carbonyl (0.55). It should be noted that the large value of the standard partial charge has been imposed to produce the correct H-bonding energies on a solely electrostatic basis with the Lennard-Jones parameters for the atoms used by MOLARIS. An alternative variable in parameterizing the C=O ligands is the size of the oxygen (i.e. an alternative Lennard-Jones 6–12 potential); for the effects of altering the partial charge can be produced to some extent by altering the 6–12 potentials. Since the well-established GROMOS [25] algorithm uses a different set of 6–12 potentials and partial charges for carbonyl oxygens than does MOLARIS, we will now examine this question by using GROMOS Lennard-Jones parameters for the ligand carbonyls.

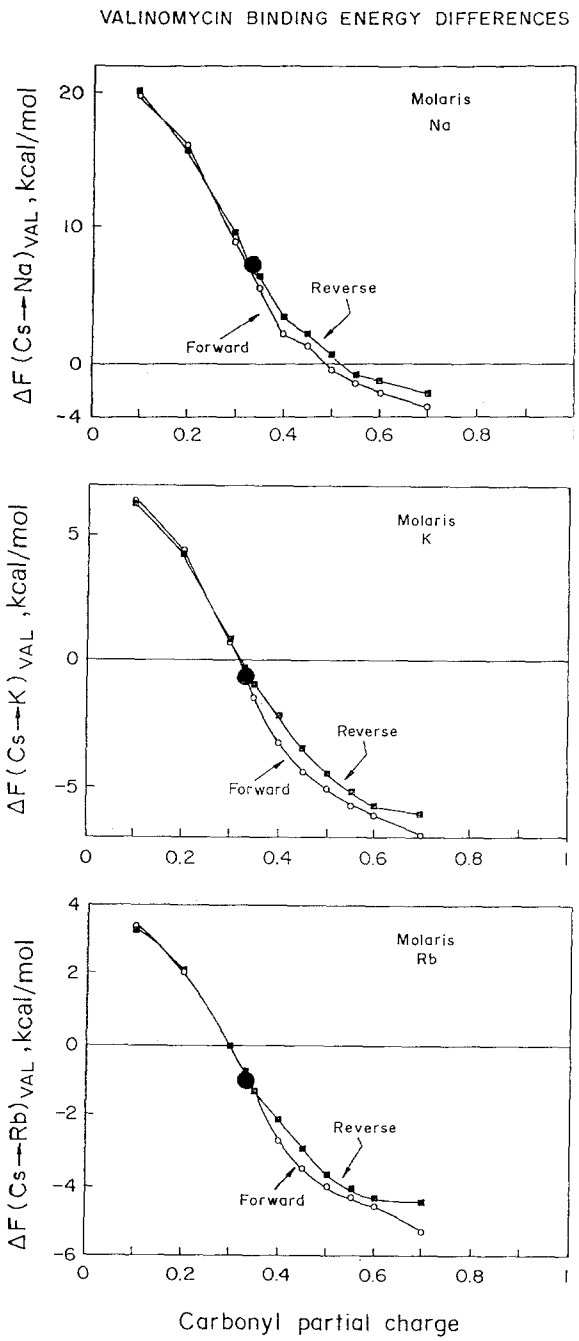

Fig. 9. Demonstration of quantitative agreement between calculated and experimentally measured selectivity for a carbonyl partial charge of 0.33 for both the forward (open circles) and reverse (filled boxes) mutations. Top: Na relative to Cs; middle: K relative to Cs; bottom: Rb relative to Cs. The large filled circles represent the experimental data.

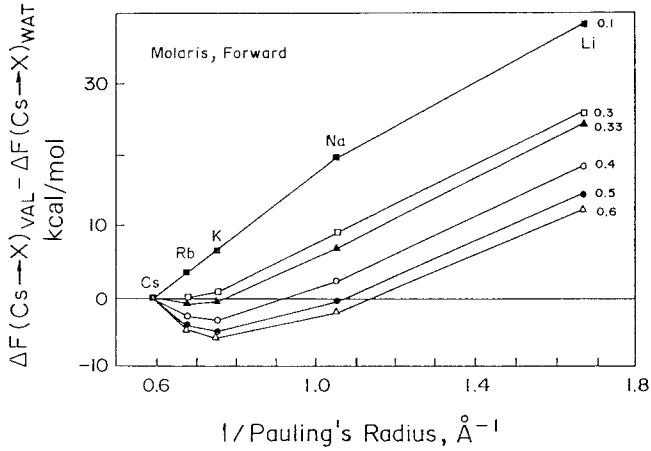

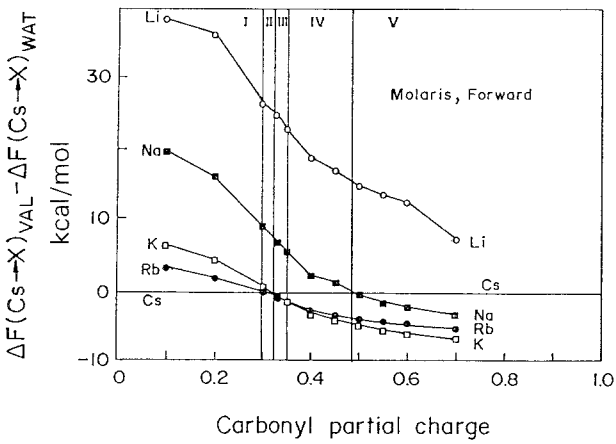

Fig. 10. Values of selectivity including Li calculated by MOLARIS for the forward mutations (Li to Na combined with Na to Cs). *Top*: plotted in the manner of Figure 7; *Bottom*: plotted in the manner of Figure 8.

4.5. AN ALTERNATIVE PARAMETERIZATION OF CARBONYL OXYGENS FOR THE MOLARIS FORCE FIELD USING GROMOS LENNARD-JONES PARAMETERS FOR THESE OXYGENS

The GROMOS program uses somewhat different Lennard-Jones 6–12 parameters for the ester carbonyl oxygens (A = 550.0, B = 23.25) than MOLARIS, defining a somewhat smaller oxygen. The valinomycin molecule offers an opportunity to compare MOLARIS with GROMOS oxygens using the MOLARIS force field. Figure 11 summarizes such computations using MOLARIS for the forward mutation using GROMOS Lennard-Jones parameters for the ester carbonyl oxygens. Figure 11 compares the experimental data with the selectivity curve for the indicated values of partial charge, including the standard GROMOS partial charge of 0.383. It is apparent that a satisfactory representation of the experimental data

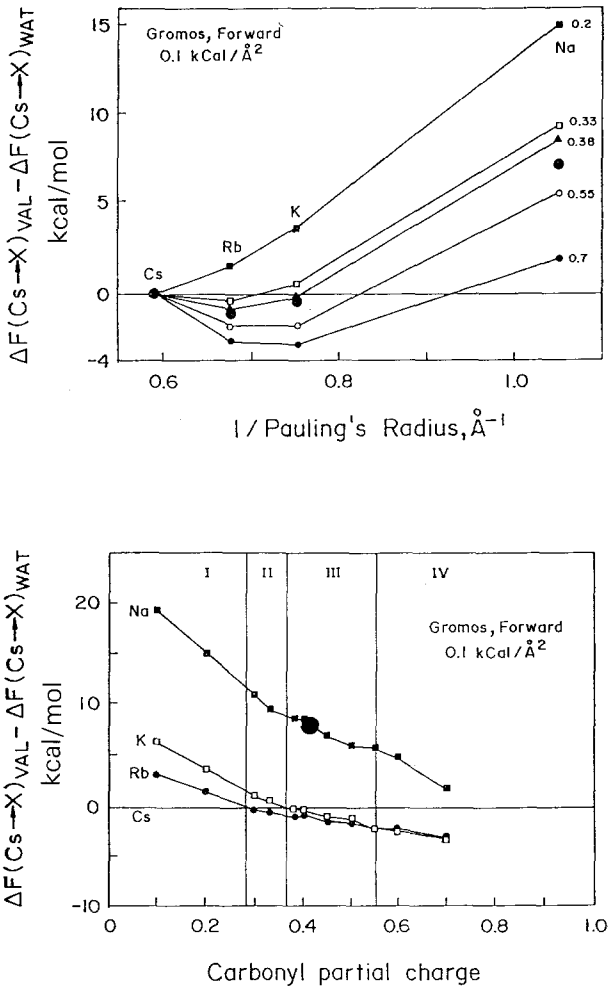

Fig. 11. Selectivity of MOLARIS using GROMOS Lennard-Jones 6–12 parameters for the ester carbonyl. *Top*: plotted in the manner of Figure 7; *Bottom*: plotted in the manner of Figure 8. Notice that the best agreement between experimental data points (large dots) and theoretical expectations would occur for a partial change around 0.41, slightly higher than the standard GROMOS value of 0.383.

can indeed be obtained for a value of partial charge around 0.41, slightly higher than the standard value for a GROMOS amide carbonyl. This is a somewhat surprising finding when combined with the conclusion that the partial charge that gives the correct selectivity is 0.33 for the *larger* GROMOS carbonyl; for intuitively one would have expected it to be *smaller* to get a comparable electric field at the surface of the oxygen. There is a simple, and highly instructive, explanation for this which will be given in the next section.

At the present stage of this work it is not possible to decide (from energetics alone) whether GROMOS or MOLARIS parameters are better to use for ions. Structurally, the ion-ligand distances and efficiency with which the carbonyl bonds points at the ion are summarized in Table IV, which will be discussed below.

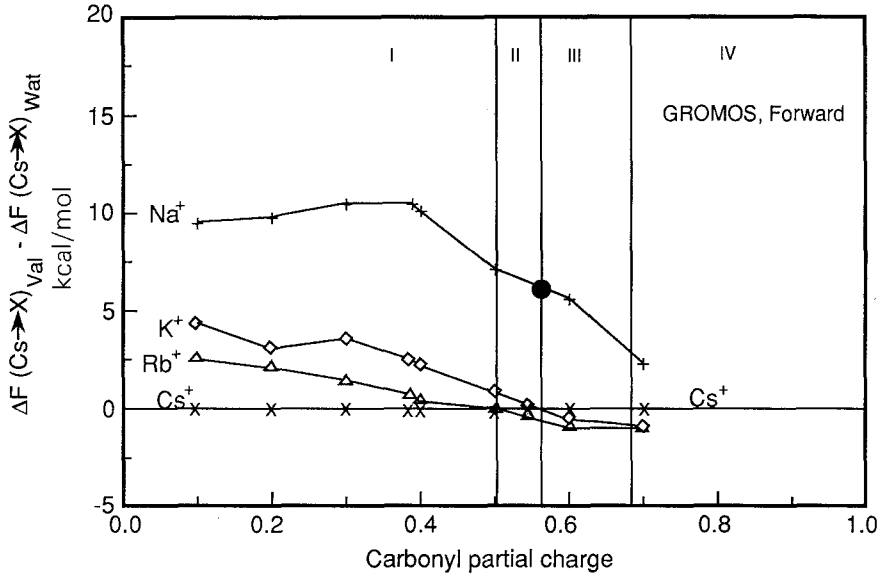

Fig. 12. Selectivity of GROMOS with extended atoms and standard parameters. The forward reaction is plotted in the manner of Figure 7. Notice that the best agreement between experimental data point (large dot) and theoretical expectations would occur for a partial charge around 0.55, somewhat higher than the standard GROMOS value of 0.383.

4.6. RECENT SIMULATIONS WITH THE GROMOS FORCE FIELD

We have very recently repeated these computations using the GROMOS force field [25] (with extended atoms) and parameters. The results are shown in Figure 12 for the forward mutation and should be compared with those of Figures 11 and 8. The overall behavior is quite similar; although the pattern of inversion of selectivity is shifted even further to the right than in Figure 11 relative to the standard MOLARIS results of Figure 8 (for GROMOS the best fit to the experimental data is seen to occur for a partial charge around 0.55).

Since FEP/MD simulations with both the MOLARIS and GROMOS force fields can successfully account for the experimental data, the use of both MOLARIS and GROMOS algorithms for evaluating ion binding to proteins is validated.

5. Structure

For the MOLARIS force field with both MOLARIS and GROMOS carbonyls we have compared the original crystallographic structure for K^+ with the energy minimized structure for K^+ snapshot generated in the molecular dynamics mutation from Na^+ to K^+. We find the backbones to be virtually identical with only slight differences between the side chains. This indicates that the host molecule neither flies apart nor collapses unreasonably. The energy minimized structures of snapshots from the FEP dynamics runs for K^+ give virtually identical results to the X-ray structure for K^+.

The energy minimized structures of snapshots for the different cations show systematic puckering of the backbone and systematic changes in the ion-oxygen

Table IV. Distances and angles between ions and ligands

		MOLARIS Carbonyl pt.chg: 0.33		GROMOS Carbonyl pt.chg: 0.41	
		Distance	Angle	Distance	Angle
Na	1	2.635	152.127	2.678	163.095
	2	2.667	157.923	2.533	166.404
	3	2.647	153.306	2.494	162.839
	4	2.686	150.817	2.731	159.840
	5	2.674	152.851	2.636	161.270
	6	2.726	155.836	3.028	160.981
K	1	2.843	147.370	2.791	157.227
	2	2.830	154.825	2.873	161.522
	3	2.805	148.518	2.787	156.973
	4	2.854	140.773	2.819	155.388
	5	2.837	147.296	2.876	157.144
	6	2.811	151.635	2.827	160.237
Rb	1	2.910	141.460	2.852	156.396
	2	2.949	155.306	2.871	159.763
	3	2.885	148.755	2.905	156.403
	4	2.931	130.010	2.862	154.552
	5	2.951	145.195	2.886	154.627
	6	2.889	149.032	2.903	159.399
Cs	1	3.051	139.631	2.973	152.615
	2	3.069	149.785	2.961	157.226
	3	3.150	110.842	3.055	155.481
	4	3.123	119.677	2.961	152.117
	5	3.120	116.349	2.988	150.566
	6	3.076	150.008	3.028	157.844

Distances (in ångstrom units) are between the ion center and the carbonyl oxygen center. The angle represents the angle between the carbonyl oxygen, the ion, and the carbonyl carbon. An angle of 180 degrees indicates that the C=0 bond points directly at the ion.

distances and angles summarized in Table IV for both MOLARIS and GROMOS carbonyl oxygens. Figure 13 compares the ion-oxygen distances for the MOLARIS carbonyls with those expected from Pauling crystal radii (straight line), the agreement is seen to be excellent for Rb^+ and Cs^+, indicating that the Lennard-Jones parameters used are appropriate. However, the agreement is less satisfactory for the smaller cations, the structure being apparently too rigid to collapse more completely around K^+ and Na^+. That these ions do not find an off-center energy minimum is surprising, though a tendency to do so does seem to exist with the smaller GROMOS carbonyls, as can be seen from Table IV. Possibly in the energy minimization procedure near absolute zero temperature we are finding the minimum potential energy conformation but missing the existence of an ensemble of 3 or 6 (symmetrical) local minima around the periphery of the cavity where the smaller ions at room temperature can transiently find minima at the closest distance of approach expected from their van der Waals sizes. Perhaps evidence in support

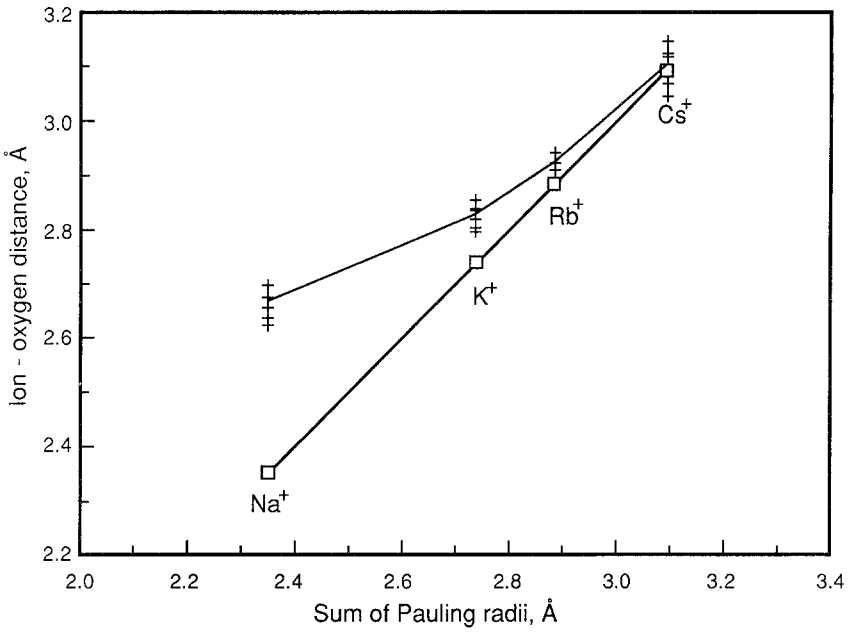

Fig. 13. Ion-carbonyl ligand distances observed in the energy minimized (40 ps at 1K) coordinates of the 'snapshots' from the FEP/MD simulations at 100 K (plotted as plus symbols) compared to the values expected according to the Pauling crystal radii (plotted as squares).

of this notion is contained in the ion-oxygen distances in the non-energy minimized snapshot for MOLARIS carbonyls with Na^+, where the distances are: 2.675, 2.714, 2.733, 2.993, 3.009, 3.075. In this transient structure, the shortest potassium–oxygen distance is quite close to the value of 2.75 Å expected from the sum of the Pauling crystal radii. This contrasts with the average distance of 2.82 Å calculated for the energy-minimized structure and plotted in Figure 13. That a low-temperature energy minimized structure might not show local minima accessible only at higher temperatures has been discussed recently by Van Gunstaren *et al.* [52].

From these results it is clear that, although 'field strength' considerations alone clearly can account for the observed selectivity sequence (see Section 6.1 of the Discussion), part of the high discrimination against Na by valinomycin is probably played by the steric inability of the molecule to achieve tight coordination without paying a substantial price in deformation energy.

5.1. ION–CARBONYL BOND ANGLES

Table IV presents for each of the cations the carbon-oxygen ion angle (in degrees) found for the MOLARIS force field with the MOLARIS and GROMOS carbonyls. This table enables one to compare the distances and angles calculated for the larger MOLARIS carbonyls with those computed for the smaller GROMOS carbonyls. The most striking observation is that the GROMOS carbonyl angle is closer to the 180 degrees expected for a carbonyl group pointing directly at the ion, an angle that

maximizes the cation-oxygen attraction and minimizes the carbon-carbon repulsion. The difference between GROMOS and MOLARIS carbonyls becomes increasingly pronounced as cation size increases (notice that for Cs three angles are less than 120 degrees for MOLARIS carbonyls, while none is less than 150 degrees for GROMOS carbonyls). This indicates that the bulkier MOLARIS ligands cannot point as favorably at the larger cations. This results in an essentially steric (bad orientation) discrimination against the larger cations for the larger MOLARIS carbonyls that disfavors these relative to the smaller ones and leads to the paradoxical crossovers, mentioned above, in selectivity sequence at lower partial charge values for the larger MOLARIS carbonyls than for the smaller GROMOS carbonyls (compare Figures 11 and 10). This has interesting implications for the interpretation of selectivity in terms of both steric and field strength contributions, as discussed in Section 6.1 and elsewhere [56].

6. Discussion

6.1. THE SELECTIVITY PATTERN

It is clear for both MOLARIS carbonyls (Figure 8) and GROMOS carbonyls (Figure 11) that the selectivity isotherms pass through the so-called Eisenman selectivity sequences [46, 47, 50] as a function of increasing partial charge. The lowest 'field strength' sequence I is seen at the extreme left. Here the Cs isotherm is the lowest (most preferred); and the sequence of selectivity is Cs > Rb > K > Na. Looking at the 'forward' mutations and proceeding to the right, the first change of sequence occurs when the partial charge is increased to about 0.3, at which point the Rb isotherm crosses the Cs isotherm; so that the sequence becomes Rb > Cs > K > Na, which is Eisenman sequence II. Proceeding further to the right, the K isotherm crosses the Cs isotherm when the partial charge is increased to about 0.32 for the MOLARIS carbonyl and 0.36 with the GROMOS carbonyl. The sequence is now Rb > K > Cs > Na, which is Eisenman sequence III, and is the one characteristic of valinomycin.

This sequence exists over a relatively narrow range for MOLARIS carbonyls and a wider range of GROMOS carbonyls since the K isotherm crosses the Rb isotherm to produce sequence IV (K > Rb > Cs > Na) at a partial charge of 0.34 for MOLARIS and 0.54 for GROMOS. Finally, at a partial charge of 0.48 for the MOLARIS carbonyl and at 0.8 (extrapolated) for the GROMOS carbonyl the Na isotherm crosses the Cs isotherm resulting in sequence V (K > Rb > Na > Cs) for this and higher values of partial charge. As noted above this is paradoxical in that the smaller carbonyl oxygen appears to require a larger partial charge to produce an equivalent 'field strength' [46, 47] effect. This illustrates a limitation of interpreting observations from real protein structures in terms of oversimplified models, as discussed elsewhere [56]. In particular, the achievement of a 'higher field strength' Eisenman sequence for a given value of partial charge by the *larger* carbonyl ligand is a consequence of discrimination *against* the larger ions rather than a favoring of the smaller ones! This explains the counter-intuitive finding noted in a preceding section that the partial charge that gives the experimentally correct selectivity is *larger* (sic) for the *smaller* GROMOS carbonyl instead of being smaller.

The same pattern of selectivity inversions is seen for the reverse mutation, though the range of partial charge over which sequence III is observed is somewhat broader. Nevertheless, when the second constraint of the proper value for the Na–Cs free energy difference is applied (see solid experimental data point), the best agreement is constrained to a partial charge of 0.33, just as in the case of the forward mutation.

The selectivity pattern can also be seen on plots of selectivity vs ion size like Figure 7. In the case of such plots, the selectivity optimum occurs at the size of the ion that is preferred [50].

6.2. PREVIOUS CALCULATIONS OF VALINOMYCIN SELECTIVITY

Theoretical calculations of the ion interactions with valinomycin were first carried out by A. Pullman *et al.* [51]. These successfully reproduced the selectivity but were based on a frozen structure (the crystallographic structure for the K-valinomycin complex) which was kept the same for all ions while the intramolecular interaction energy was computed by optimizing the position of the cation inside the (rigid) cavity. Such calculations are interesting but do not reflect the ability of valinomycin to adjust its structure to relieve local strains. This is not a trivial matter. In calculations on gramidicin [6] and on viral ion binding sites [4, 16] it was found that using a fixed structure causes a large component of the selectivity to be attributed to steric effects (e.g. van der Waals repulsion) which should become completely negligible in a structure that can relax.

Comparing Pullman's minimum ion-ligand distances with Pauling radii, it is apparent that all her ions are too small, being approximately shifted by one ion towards Li. In particular, her Rb radius corresponds to that observed for K. Therefore, Rb will be the ion that fits best in the K crystal structure; and the correct selectivity apparently emerges as a consequence of using too small ions in a rigid structure, a situation not too dissimilar to the conclusions previously reached in primitive modelling of a frozen viral selectivity filter [18].

It will be interesting to compare the energies of the optimized valinomycin and viral structures with those of the frozen structures. The subject of selectivity in 'frozen' vs. rearrangeable structures has been discussed in general terms [13, 22, 38, 53] and is examined in detail elsewhere [56] for valinomycin.

Another example of the importance of extending selectivity modelling to include the energetics of structural rearrangement has been given in Section 6.1. Here the paradoxical finding of an effectively higher 'field strength' for a given partial charge imbedded in a larger carbonyl oxygen than in a smaller one was rationalized by recognizing a 'steric' contribution.

6.3. SOME COMMENTS ON ISOSTERICITY

A few comments are now in order on the question of whether or not isostericity can strictly exist in a protein when replacing one ion by another and on the related question of whether or not a strictly isomorphous replacement is ever possible between ions. There is a large body of spectroscopic data germane to this (see pp. 127–131 of [39] and 19–24 of [54] for discussion and references); but to discuss

these exceeds the scope of the present paper. From the preceding Section 5 it should be apparent that, despite the apparently isosteric behavior of the experimental data, valinomycin *does* change its structure slightly to accommodate the different sized ions; and this has important energetic consequences. A useful analogy can be made with a system of springs. The van der Waals repulsion term represents a very stiff spring (12th power spatial dependence) while the other interactions between protein atoms represent much weaker springs. In a strictly frozen system in which an ion replaces another isomorphously the only species dependent contribution to selectivity comes from van der Waals interactions between the ion and the ligands (see [53, 56] for details). In such a system selectivity has a purely steric origin. But we would argue that this can never happen in a real protein since small readjustments will relieve the van der Waals strain, essentially distributing it over a somewhat larger region. For example consider what actually occurs when an ion that fits easily into the natural cavity of valinomycin (e.g. Na^+) is replaced by a larger ion (e.g. Cs^+). In a rigid structure this would imply a large van der Waals repulsive energy; but what actually happens [56] is that the van der Waals strain is released by compressing the weaker springs that constitute the bond and non-bond interactions between all the other atoms of the protein (bond stretching, bond-angle bending, torsional-angle contributions, and intramolecular charge-charge and VDW interactions). In this way the repulsive charge effect of differing ion size is distributed over a larger group of atoms than the immediate neighbors, which of course implies that the replacement cannot be strictly isomorphous. The experimentally observed 'isostericity' in this case is therefore only approximate and signifies that the changes in structure are relatively localized so that the overall shape and size of the complex are not altered significantly thereby. In the literal sense, strict isostericity between ions and strictly isomorphous replacements can never occur in a protein!

7. Summary and Conclusions

Rationale. Studies of two-phase salt extraction equilibria underlying the ability of valinomycin to extract the picrates and dinitrophenolates of Cs^+, Rb^+, K^+, Na^+, Li^+, Tl^+, and NH_4^+ from aqueous solutions into organic phases (dichloromethane, *n*-hexane, and their mixtures) have shown that the valinomycin–ion complexes of most of these ions are quite isosteric. For isosteric complexes the *differences* in free energy between the different ions are expected to be independent of the solvent in which the complex exists. Such free energy *differences* correspond to *ratios* which are the usual measures of selectivity. Experimentally it is found that the ratios of two-phase equilibrium constants relative to Cs^+ agree closely with the ratios of the homogeneous equilibrium constants for ion-complex formation in methanol, as well as with ratios of conductance and permeabilities in lipid bilayers, and even with selectivity coefficients of bulk ion-selective electrodes. These observations imply that isostericity of ion-valinomycin complexes both for media ranging in polarity from hexane to methanol. This is strictly true for K^+, Rb^+, Cs^+, Tl^+, and NH_4^+, approximately true for Na^+, but breaks down for Li^+. The property of isostericity enables meaningful theoretical calculations to be carried out *in vacuo* since the *differences* in calculated free energy can be directly compared with those measured

experimentally, regardless of the media in which they were measured. This provides an opportunity to test the GROMOS and MOLARIS force fields and parameters against experimental data.

Measurements. Precise ion selectivity ratios were measured by two-phase salt extraction into dichloromethane and compared with ratios measured for bilayers and for the homogeneous complexation reaction in methanol. All observed ratios are found to exist in the Eisenman selectivity sequence III: Rb > K > Cs ≫ Na > Li. The 2-phase salt extraction measurements into dichloromethane yield the most accurate free energy differences. These are (in kcal/mol referred to Cs in the aqueous reference state): Rb: −1.2; K: −0.75; Cs: 0.0; Na: +6.89; Li: +8.42.

Simulations. These values were compared with those calculated *in vacuo* by FEP/MD simulations for the valinomycin-alkali cation complexes carried out for both the MOLARIS and GROMOS force fields starting with the crystallographic atomic coordinates of the K–valinomycin complex using Lennard-Jones 6–12 parameters for the ions derived from aqueous solution data. On the one hand, for the standard partial charges and Lennard-Jones parameters of MOLARIS, the calculations predict the selectivity sequence K > Rb > Na > Cs > Li. This is Eisenman sequence V, which would be expected for a binding site having a field strength stronger than that of valinomycin. On the other hand, for the standard partial charges and Lennard-Jones parameters of GROMOS the predicted selectivity sequence is Cs > Rb > K > Na > Li. This is the lyotropic sequence (Eisenman sequence I) and would be expected of a binding site having a field strength weaker than that of valinomycin.

Parameterization of ester carbonyl and comparison of simulations with experiments. Despite these differences we show that it is possible with both GROMOS and MOLARIS force fields to fit the experimental data both as to sequence (Rb > K > Cs ≫ Na > Li) and magnitude (particularly the large preference of K, Rb, and Cs relative to Na (6.89 kcal/mol Cs preference over Na)). This is accomplished if one parameterizes the partial charges of the ester carbonyl ligands appropriately. When this is done, FEP/MD simulations using either the MOLARIS or GROMOS force fields give quantitative fits to the experimental data. We conclude that these two fields are valid as appropriate procedures for computing ion binding selectivity in proteins.

Acknowledgement

The research was supported by USPHS Grant GM 24749, by the Swedish Natural Science Research Council (NFR), and by FONDECYT GRANT 1112-1989. We thank Emily Maverick for the Cambridge Data Base structures for valinomycin, Rich Little for help in programming and analyzing ligand distances and bond angles, and Fred Lee for help in customizing MOLARIS and in preparing the library entries for lactate and hydroxyisovalerate.

References

1. C. J. Pedersen: *J. Am. Chem. Soc.* **89**, 7017 (1967).
2. G. Eisenman, S. Ciani and G. Szabo: *Federation Proceedings* **27**, 1289 (1968).

3. C. J. Pedersen: *Federation Proceedings* **27**, 1305 (1968).
4. G. Eisenman, S. Ciani and G. Szabo: *J. Membr. Biol.* **1**, 294 (1969).
5. G. Eisenman, G. Szabo, S. G. A. McLaughlin and S. M. Ciani: in *Symposium on Molecular Mechanics of Antibiotic Action on Protein Biosynthesis and Membranes*, eds. E. Munoz, F. G. Ferrandiz and D. Vasquez, Elsevier, Amsterdam, London, New York (1972), pp. 545–602.
6. G. Eisenman, G. Szabo, S. Ciani, S. McLaughlin and S. Krasne: in *Progress in Surface and Membrane Science* **6**, 139 (1973) Academic Press, New York.
7. S. McLaughlin, G. Szabo, S. Ciani, and G. Eisenman: *J. Membr. Biol.* **9**, 3 (1972).
8. J. A. McCammon, P. G. Wolynes and M. Karplus: *Biochemistry* **18**, 927 (1979).
9. A. Warshel, and J. Aqvist: in *Theoretical Biochemistry and Molecular Biophysics*, eds. D. L. Beveridge and R. Lavery, Adenine Press (1990), pp. 1–18.
10. B. R. Brooks, R. E. Brucoleri, B. D. Olafson, D. J. States, S. Swaminathan and M. Karplus: *J. Comp. Chem.* **4**, 187 (1983).
11. P. K. Weiner and P. A. Kollman: *J. Comp. Chem.* **2**, 287 (1981).
12. W. F. van Gunsteren and P. K. Weiner: *Computer Simulation of Biomolecular Systems*, Escom, Leiden (1989).
13. J. Åqvist and A. Warshel: *Biophys. J.* **56**, 171 (1989).
14. S. Furois-Corbin and A. Pullman: in *Transport Through Membranes: Carriers, Channels and Pumps*, eds. A. Pullman, J. Jortner and B. Pullman, Kluwer Academic Publishers, Dordrecht, Boston, London (1988), pp. 337–357.
15. S. Furous-Corbin and A. Pullman: *Fed. Eur. Biochem. Soc.* **252,** 63 (1989).
16. G. Eisenman, A. Villarroel, M. Montal and O. Alvarez; in *Progress in Cell Research*, eds. J. M. Ritchie, P. J. Magestretti and L. Bolis, Elsevier (1990), Vol. 1, pp. 195–211.
17. A. M. Silva, R. E. Cachau and D. J. Goldstein: *Biophys. J.* **52**, 595 (1987).
18. G. Eisenman, A. Oberhauser and F. Bezanilla: in *Transport Through Membranes: Carriers, Channels and Pumps*, eds. A. Pullman, J. Jortner, B. Pullman, Kluwer Academic Publ. Dordrecht, Boston, London (1988), pp. 27–50.
19. F. Sussman and Harel Weinstein: *Proc. Nat. Acad. Sci. USA* **86**, 7880 (1989).
20. G. Wipff, and J. M. Wurtz: in *Transport Through Membranes: Carriers, Channels and Pumps*, eds. A. Pullman, J. Jortner, B. Pullman, Kluwer Academic Publishers, Dordrecht, Boston, London (1988), pp. 1–26.
21. P. D. J. Grootenhuis and P. A. Kollman: *J. Am. Chem. Soc.* **111**, 4046 (1989).
22. G. Eisenman and O. Alvarez: in *Ca Transport and Homeostasis*, ed. D. Pansu, NATO ASI Series, vol H48, Springer Verlag, Berlin, New York, Tokyo (1990), p. 283.
23. J. Åqvist and A. Warshel: *J. Am. Chem. Soc.* **112**, 2860 (1990).
24. S. J. Weiner, P. A. Kollman, D. T. Nguyen and D. A. Case: *J. Comp. Chem.* **7**, 230 (1986).
25. W. F. Van Gunsteren, H. J. C. Berendsen, J. Hermans, W. G. J. Hol and J. P. M. Postma: *Proc. Natl. Acad. Sci. USA* **80**, 4315 (1983).
26. J. Åqvist, W. F. van Gunsteren, M. Leijonmarck and O. Tapia: *J. Mol. Biol.* **183**, 461 (1985).
27. A. T. Brunger, R. L. Campbell, G. M. Clore, A. M. Gronenborn, M. Karplus, G. A. Petsko and M. M. Teeter: *Science* **235**, 1049 (1987).
28. J. Åqvist: *J. Phys. Chem.* **94**, 8021 (1990).
29. R. H. Kretzinger: *CRC Crit. Rev. Biochem.* **8**, 119 (1980).
30. G. Eisenman and J. A. Dani: *Ann. Rev. Biophys. Biophys. Chem.* **16**, 205 (1987).
31. O. Herzberg and M. N. G. James: *Biochem.* **24**, 5289 (1985).
32. T. A. Jones and L. Liljas: *J. Mol. Biol.* **177**, 735 (1984).
33. I. Montelius, L. Liljas and T. Unge: *J. Mol. Biol.* **201**, 353 (1988).
34. D. W. Urry: *Proc. Natl. Acad. Sci. U.S.A.* **68**, 672 (1971).
35. B. A. Wallace and K. Ravikumar: *Science* **241**, 182 (1988).
36. A. Warshel and S. Creighton: in *Computer Simulation of Biomolecular Systems*, eds. W. F. van Gunsteren and P. K. Weiner, Escom, Leiden (1989), pp. 120–137.
37. A. Warshel, F. Sussman and G. King: *Biochemistry* **25**, 8368 (1985).
38. G. Eisenman and A. Villarroel: in *Monovalent Cations in Biological Systems*, ed. C. A. Pasternak, CRC Press Publishers. Boca Raton, FL (1989), pp. 1–29.
39. Y. A. Ovchinnikov, V. T. Ivanov and A. M. Shkrob: *BBA Library*, Elsevier Scientific Publ. Co., Amsterdam, Oxford, New York (1974), Vol. 12 pp. 1–464.

40. Neupert-Laves and M. Dobler: *Helv. Chim. Acta* **58**, 432 (1975).
41. L. K. Steinrauf and K. Folting: *Isr. J. Chem.* **24**, 290 (1984).
42. L. K. Steinrauf, J. A. Hamilton, and M. N. Sabesan: *J. Am. Chem. Soc.* **104**, 4085 (1982).
43. E. Grell, T. Funck and F. Eggers: in *Membranes*, ed. G. Eisenman, Dekker, New York (1975), Vol. 3. Ch. 1. pp. 1–126.
44. P. Mueller and D. O. Rudin: *Biochem. Biophys. Res. Commun.* **26**, 398 (1967).
45. L. A. R. Pioda, V. Stankova and W. Simon: *Anal. Letters.* **2**, 665 (1969).
46. G. Eisenman: in *Symposium on Membrane Transport and Metabolism*, eds. A. Kleinzeller and A. Kotyk, Academic Press, New York (1961), pp. 163–179.
47. G. Eisenman: *Biophys. J.*, **2**, (2), 259 (1962).
48. J. Burgess: *Metal ions in Solution*. Ellis Horwood Ltd. Chicester, England (1977) p. 186.
49. R. W. Zwansig: *J. Chem. Phys.* **22**, 1420 (1954).
50. G. Eisenman and R. Horn: *J. Membr. Biol.* **76**, 197 (1983).
51. N. Gresh, C. Etchebest, O. de la luz Rojas and A. Pullman: *Int. J. Quantum Chem: Quantum Biol. Symp.* **8**, 109 (1981).
52. W. F. Van Gunstaren, P. Gros, and A. E. Torda: *Abstr. 10th Int. Biophys. Congress* (1990), p. 11.
53. G. Eisenman, and O. Alvarez: *J. Membr. Biol.* **119**, 109 (1991).
54. K. Easwaran: in *Ion Treatment Through Membranes*, ed. K. Yagi and B. Pullman, Academic Press, Tokyo, New York (1987) pp. 17–39.
55. G. Eisenman: *Excerpta Medica, Int. Congr. Ser.* No. 87, 489 (1965).
56. G. Eisenman, and O. Alvarez: in *Membrane Structure and Function: The State of the Art*, K. R. K. Easwaran and B. P. Gaber, eds. Adenine Press, New York (1991). In Press.